# Host B7x Promotes Pulmonary Metastasis of Breast Cancer

**Yael M. Abadi,[1] Hyungjun Jeon,[1] Kim C. Ohaegbulam, Lisa Scandiuzzi, Kaya Ghosh, Kimberly A. Hofmeyer, Jun Sik Lee,[2] Anjana Ray, Claudia Gravekamp, and Xingxing Zang**

**B7x (B7-H4 or B7S1) is an inhibitory member of the B7 family of T cell costimulation. It is expressed in low levels in healthy peripheral tissues, such as the lung epithelium, but is overexpressed in a variety of human cancers with negative clinical associations, including metastasis. However, the function of B7x in the context of cancer, whether expressed on cancer cells or on surrounding "host" tissues, has not been elucidated in vivo. We used the 4T1 metastatic breast cancer model and B7x knockout (B7x $^{-/-}$) mice to investigate the effect of host tissue–expressed B7x on cancer. We found that 4T1 cells were B7x negative in vitro and in vivo, and B7x$^{-/-}$ mice had significantly fewer lung 4T1 tumor nodules than did wild-type mice. Furthermore, B7x$^{-/-}$ mice showed significantly enhanced survival and a memory response to tumor rechallenge. Mechanistic studies revealed that the presence of B7x correlated with reduced general and tumor-specific T cell cytokine responses, as well as with an increased infiltration of immunosuppressive cells, including tumor-associated neutrophils, macrophages, and regulatory T cells, into tumor-bearing lungs. Importantly, tumor-associated neutrophils strongly bound B7x protein and inhibited the proliferation of both CD4 and CD8 T cells. These results suggest that host B7x may enable metastasizing cancer cells to escape local antitumor immune responses through interactions with the innate and adaptive immune systems. Thus, targeting the B7x pathway holds much promise for improving the efficacy of immunotherapy for metastatic cancer.** *The Journal of Immunology*, **2013, 190: 3806–3814.**

Metastasis is the most clinically challenging aspect of cancer. The majority of cancer-related deaths are not due to primary tumors, which are amenable to treatment, but to metastases, which are difficult to detect early and even harder to eradicate. Metastasis is an inefficient process consisting of a series of rate-limiting steps (1). Tumor cells must break away from the primary tumor, invade blood vessels, survive in the circulation, leave the bloodstream and enter tissues, and start growing into metastatic colonies. All of these steps must occur for metastasis to happen. There is currently an intense effort to understand the pathways that promote cancer metastasis so as to identify therapeutic targets and develop strategies against metastasis.

Among the many factors that are necessary for the establishment of metastases is an immunosuppressive secondary site. Once metastasizing cells have successfully left the primary tumor and entered and survived the circulation, they arrest in tissue and attempt to proliferate. These cells often develop into micrometastases that can further grow into independent tumors, but this depends largely on interactions between these cells and their new environment (1). The immune system plays an important role in these processes. In addition to infiltration by effector immune cells attempting to mount antitumor responses, growing metastases are inundated by immunosuppressive cells and molecules that enable tumor cells to escape destruction by the immune system (2–4). To design immunotherapies that are effective in metastatic cancers, it is necessary to understand the pathways involved in promoting tumor immunosuppression (5), particularly in the metastatic site.

B7x (B7-H4 or B7S1) is a recently discovered protein that is overexpressed in numerous human cancers and, in many cases, correlates with negative clinical outcome (6–21). B7x expression in renal cell carcinoma and tumor vasculature is associated with cancer progression and survival (6, 14). Prostate cancer patients with strong expression of B7x by tumor cells are significantly more likely to have disease spread and are at increased risk for clinical cancer recurrence and cancer-specific death (15). In human gastric cancer, tumor expression of B7x predicts poor survival (17). Similar findings were also reported in studies of ovarian cancer and lung cancer (10, 21). Among the negative clinical associations of B7x is increased metastasis, itself a strong predictor of mortality, as was found in lung, kidney, prostate, and gastrointestinal cancers (10, 14, 15, 17, 18, 20).

Although there is a growing literature on B7x expression and associations in cancer, little is known regarding the particular functions of B7x in the context of cancer. An inhibitory member of the B7 family of T cell costimulation, B7x binds activated T cells and inhibits proliferation and cytokine production in vitro (22–24). In contrast to classical B7 family members B7-1 and B7-2, which are expressed on APCs in lymphoid organs, B7x is expressed on nonimmune cells in peripheral tissues (12, 25–27). We initially observed relatively high B7x mRNA expression in murine lung (22) and recently found that this extends to protein expression. Specifically, we found that normal mouse lung tissue shows expression of B7x protein on epithelial cells but not on immune cells (25, 27).

Department of Microbiology and Immunology, Albert Einstein College of Medicine, Bronx, NY 10461

[1]Y.M.A., and H.J. contributed equally to this work.

[2]Current address: Department of Biology, College of Natural Science, Chosun University, Gwangju, South Korea.

Received for publication August 29, 2012. Accepted for publication February 1, 2013.

This work was supported, in part, by Department of Defense Grant PC094137 and National Institutes of Health Grant DP2DK083076. Y.M.A., K.C.O., K.G., and K.A.H. were supported by National Institutes of Health Training Grants T32GM007491, GM007288, T32DK007218, and T32DK007513, respectively. The Albert Einstein Cancer Center is supported by National Institutes of Health Grant P30CA013330.

Address correspondence and reprint requests to Dr. Xingxing Zang, Department of Microbiology and Immunology, Albert Einstein College of Medicine, 1300 Morris Park Avenue, Forchheimer Building, Room 405, Bronx, NY 10461. E-mail address: xing-xing.zang@einstein.yu.edu

Abbreviations used in this article: DC, dendritic cell; MDSC, myeloid-derived suppressor cell; TAN, tumor-associated neutrophil; Treg, regulatory T cell; wt, wild-type.



www.jimmunol.org/cgi/doi/10.4049/jimmunol.1202439

The localization of B7x and its ability to inhibit activated T cells suggest a role in modulating T cell responses on site in the periphery. Furthermore, there is some clinical evidence linking B7x expression in cancer to reduced T cell infiltration into tumors (7, 10, 19, 21, 28). These data suggest a potential protumor function for B7x through the reduction of antitumor immune responses. B7x overexpression in cancer may be a mechanism of tumor immune evasion that results in increased survival and metastasis of cancer cells. However, this has yet to be proven in an in vivo cancer model.

In addition to B7x overexpression in tumor cells, B7x is expressed at low levels in some normal peripheral tissues. We wondered whether the presence of B7x in particular organs, independent of that expressed on tumor cells themselves, played a role in supporting metastatic growth by biasing the immunological milieu of a metastatic site toward immunosuppression. Therefore, we investigated the role of B7x in a cancer model, focusing specifically on B7x expressed in nontumor, "host" tissue cells. Because B7x is expressed in the lung, we used a B7x knockout ($B7x^{-/-}$) mouse and 4T1, a B7x negative lung metastasis model, and found that $B7x^{-/-}$ mice had reduced lung metastasis, more potent effector immune responses, and fewer regulatory T cells (Tregs), macrophages, and tumor-associated neutrophils (TANs) compared with wild-type (wt) mice. Surprisingly, we found that B7x strongly bound TANs, which could suppress proliferation of both CD4 and CD8 T cells. This study suggests that host B7x may be a factor in organs, such as lung, which promotes growth of metastases through immunosuppressive functions.

## Materials and Methods

### *Animals*

$B7x^{-/-}$ mice, which were described previously (26), were backcrossed to BALB/c mice for >10 generations. Age- and sex-matched BALB/c mice were purchased from the National Cancer Institute (Fredrick, MD) and The Jackson Laboratory (Bar Harbor, ME). Mice were maintained under specific pathogen–free conditions at the Albert Einstein College of Medicine, and experiments were performed according to Institutional Animal Care and Use Committee guidelines.

### *Cell lines and stimulation*

The 4T1 cell line was derived from a spontaneous mammary carcinoma in a BALB/c mouse (29) and cultured in DMEM containing 10% FBS and 0.4 U/ml insulin. A total of $10^5$ 4T1 cells was injected for experimental metastasis and mechanism experiments. For survival studies, $10^5$ 4T1 cells were injected initially, and $2 \times 10^5$ 4T1 cells were injected for rechallenge. Thy1.1/MSCV vector was used to generate retrovirus and then transfected into 4T1 cells; $Thy1.1^+$ 4T1 cell transfectants, Thy1.1/4T1, were sorted by FACS using an anti-Thy1.1 mAb. A total of $10^5$ Thy1.1/4T1 cells was injected into mice. Human cell lines (HL60, AP-1060, Jurkat, Raji, and HeLa) were cultured in complete RPMI 1640, with the exception of AP-1060 cells, which were cultured in complete RPMI 1640 with 5% A5637 cell–conditioned media (30). For in vitro stimulation, 4T1 cells were incubated with IFN-γ (10 and 100 ng/ml) for 24–72 h. The expression of B7x and PD-L1 was then measured by FACS.

### *RT-PCR*

RNA was isolated from tissue using the TRIzol system (Sigma) and converted to cDNA using the ImProm-II system (Promega). Primers for B7x cDNA or β-actin were used in PCR to detect B7x expression.

### *Experimental lung metastasis quantification*

Mice were sacrificed and injected intratracheally with 15% India ink (Sigma). Lungs were excised and fixed/destained overnight in Fekete's solution (31), and surface nodules were enumerated under a dissecting microscope.

### *Cell isolation and flow cytometry*

Following mouse anesthetization and perfusion with PBS, lungs and spleens were digested using GentleMACS (Miltenyi Biotec) or frosted glass. After RBC lysis, filtered cell suspensions were resuspended in FACS buffer (0.5% BSA in PBS) or, for coculture experiments, in sterilized MACS buffer (0.5% BSA, 2 mM EDTA in PBS). In coculture experiments, T cells were purified from lung using Thy1.2 MACS beads (Miltenyi Biotec) in sterile MACS buffer. Cells were incubated with anti-mouse CD16/32 (eBioscience) to block FcRs and then stained with the following biotin- or fluorophore-conjugated anti-mouse mAbs: anti-B220, B7-H4 (clone 9), PD-L1, CD11b, CD11c, CD4, CD45, CD49b (clone Dx5), CD8α, F4/80, Foxp3 (clone FJK-16s), GR1 (clone RB6-8C5), IFN-γ, streptavidin, and TNF-α (all from eBioscience); anti-CD4, CD11b, Ly6G (clone 1A8), and Ly6C (all from Becton Dickinson Biosciences); or F4/80–Alexa Fluor 647 (Abd Serotec). For intracellular staining, cells were permeabilized using the Foxp3 staining buffer set (eBioscience). Samples were acquired on a FACSCalibur, LSR II, or LSR II yellow (Becton Dickinson Biosciences) and analyzed with FlowJo software (TreeStar). Cells were gated on live cells using forward scatter and Live/Dead marker (Molecular Probes) and then on $CD45^+$ cells, followed by additional lineage markers.

### *Intracellular cytokine staining*

Cells were stimulated at 37°C for ~6 h with 0.5 or 1 μg/ml PMA (Enxo Life Science International) and 1.87 μg/ml ionomycin (Sigma) in the presence of GolgiStop (Becton Dickinson Biosciences) and monensin (Sigma). Cells were washed; Fc blocked; stained with CD4, CD8, and Live/Dead marker; permeabilized; and stained with anti–IFN-γ, TNF-α, or isotype controls in permeabilization buffer for 30 min.

### *Tumor-specific cytokine stimulation*

Bone marrow cells were isolated from the femur and tibia of naive mice and cultured in complete RPMI 1640 containing GM-CSF and IL-4 (20 ng/ml each; Becton Dickinson Biosciences), which was replaced every other day, for 6 d to generate dendritic cells (DCs). Cells were incubated for an additional day with 200 ng/ml LPS and 4T1 lysate, generated through three freeze/thaw cycles. Loaded DCs were incubated for 18 h with cell suspensions from lungs of day-18 mice injected i.v. with 4T1. GolgiPlug (Becton Dickinson Biosciences) was added during the last 4 h, and cells were stained extracellularly and for cytokine production as above.

### *T cell and neutrophil coculture assays*

T cells were purified from naive spleen using Thy1.2 MACS beads (Miltenyi Biotec) and labeled with CFSE (Invitrogen) at a final concentration of 2.5 μM. Neutrophils were isolated from bone marrow or lung by labeling single-cell suspensions with FITC-conjugated Ly6G Ab (Becton Dickinson Biosciences), followed by positive selection using FITC MACS beads. Purity was generally >90%. Neutrophils and T cells were cocultured in complete RPMI 1640 in 96-well round-bottom plates coated with 5 μg/ml anti-CD3 (145-2C11; eBioscience). After 4 d, cells were labeled and acquired by FACS. Proliferation index was calculated using FlowJo software (32).

### *Cytospin*

$Ly6G^{hi}$ cells were sorted using a FACSAria (Becton Dickinson Biosciences), resuspended in PBS with 10% FBS, centrifuged in a Cytospin 2 (Shandon), stained with Harris hematoxylin (Fisher), and photographed using a COOLSCOPE Digital camera (Nikon).

### *Histology*

Lungs were fixed in zinc fixative (Becton Dickinson Pharmingen) and embedded in paraffin. Five-micron sections were stained with Harris H&E (Poly Scientific) and photographed using a COOLSCOPE camera.

### *Ig fusion proteins*

B7x-Ig and control Hu-IgG were generated as previously described (22). MACS-purified neutrophils or total cell suspensions were incubated with 1 μg/100 μl Ig protein for 45 min on ice. Cells were washed, incubated with fluorophore-conjugated anti-human IgG Fcγ (Jackson ImmunoResearch) for 30 min, and acquired by FACS.

### *Statistics*

Statistical analysis was performed with Prism software (GraphPad), using the unpaired Student *t* test or the log-rank test (survival studies), with results typically displayed as mean ± SEM. The $p$ values $< 0.05$ were considered statistically significant.

## Results

### *B7x deficiency protects mice from experimental lung metastasis*

We recently showed that B7x protein is detected on the bronchial epithelium of the lung (25) but not on any cells of hematopoietic

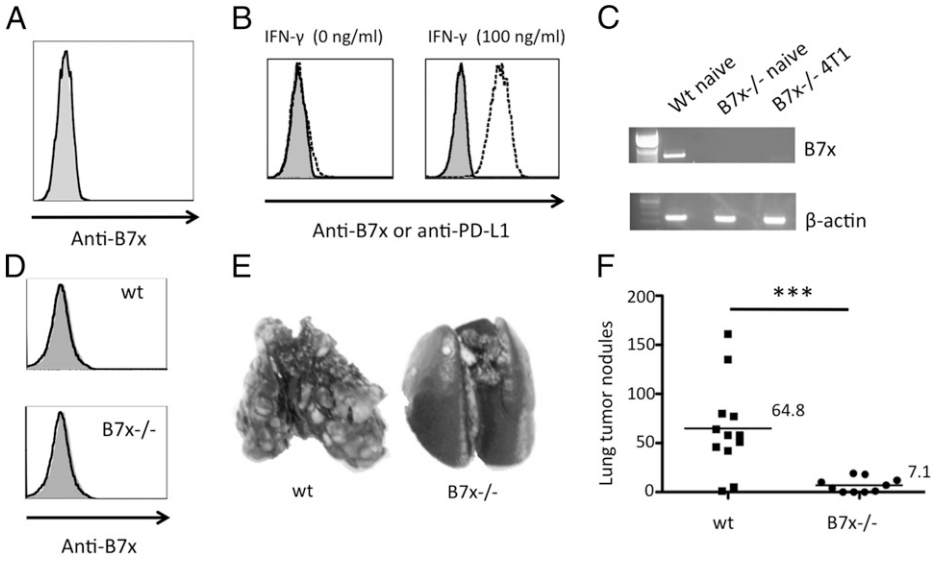


**FIGURE 1.** 4T1 cells are B7x negative, and B7x knockout mice have reduced lung metastasis of 4T1. (**A**) 4T1 cells were stained with anti-B7x (open graph) or isotype control (shaded graph). (**B**) 4T1 cells were stimulated with IFN-γ (100 ng/ml) for 3 d and then stained with anti-B7x (open graph), anti–PD-L1 (dashed line), or isotype control (shaded graph). (**C**) RT-PCR of mRNA isolated from naive or 4T1 metastatic lung. (**D**) Thy1.1$^+$ cells (4T1) from lungs of wt and B7x$^{-/-}$ mice injected via the tail vein with Thy1.1/4T1 were stained with anti-B7x (open graph) or isotype control (shaded graph). Lung metastases resulting from tail vein 4T1 injection; representative lungs after India ink injection (**E**) and lung tumor nodule counts (**F**) pooled from two independent experiments ($n$ = 10–12). ***$p < 0.001$.

origin or lymphoid tissues (25–27). Therefore, we used B7x$^{-/-}$ mice on a BALB/c background and a syngeneic pulmonary metastasis model, 4T1, to explore the effect of tissue-expressed B7x on cancer metastasis. Like naive B7x$^{-/-}$ mice on a 129 background (26), naive BALB/c B7x$^{-/-}$ mice had no apparent phenotype and had normal numbers and distribution of immune cells. 4T1 is an aggressive, highly metastatic mammary carcinoma cell line that spontaneously metastasizes to lung (29). We first ascertained that 4T1 cells did not express B7x so as to preclude recognition of B7x as a foreign Ag in B7x$^{-/-}$ mice. 4T1 cells did not express B7x in vitro (Fig. 1A). This did not change upon stimulation with IFN-γ. Although IFN-γ stimulation was able to upregulate PD-L1 expression on 4T1 cells, it had no effect on B7x expression (Fig. 1B). Furthermore, 4T1 tumors did not express B7x in vivo. RT-PCR of mRNA isolated from 4T1 metastatic lung of B7x$^{-/-}$ mice did not detect B7x expression (Fig. 1C). Finally, we injected Thy1.1/4T1 cells i.v. into mice and found that Thy1.1$^+$ cells (4T1) from metastatic lung of wt and B7x$^{-/-}$ mice were B7x$^-$ (Fig. 1D). Thus, 4T1-induced pulmonary metastasis in B7x$^{-/-}$ and wt mice was a suitable model for our study of the effects of B7x expressed in the tissue of the metastatic site.

B7x$^{-/-}$ and wt mice were injected i.v. in the tail vein with 4T1 in an experimental metastasis study, in which tumor cells deposited in the circulation are transported to the heart and frequently arrest in the lungs. By day 17 or 18 post-i.v. injection, wt mice appeared sick, and all mice were sacrificed. We evaluated the lungs of these mice for metastatic nodules and found that numerous tumor nodules were visible on the surface of the lungs of wt mice, whereas B7x$^{-/-}$ mice had significantly fewer lung nodules (Fig. 1E, 1F). The average number of lung tumor nodules in wt mice was ~9-fold higher than that in B7x$^{-/-}$ mice (64.8 in the wt group versus 7.1 in the B7x$^{-/-}$ group). Because the only difference between these two groups of mice was tissue expression of B7x, such as in the lung, these results suggest that local B7x expression was sufficient to support and promote the growth of metastatic colonies arising from cancer cells reaching the lungs.

### *B7x knockout mice can survive 4T1 challenge and generate memory response*

Survival studies were also conducted using the 4T1 tail vein model. In agreement with the lung tumor nodule results, B7x$^{-/-}$ mice had a significantly lower death rate than did wt mice. By day 33 postinjection, 100% of wt mice were dead, whereas only 26% of B7x$^{-/-}$ mice had died. At the end of 10 wk, one third of the B7x$^{-/-}$ mice were still alive and appeared healthy (Fig. 2A). We investigated whether the surviving B7x$^{-/-}$ mice had generated a memory response to 4T1. These B7x$^{-/-}$ mice were rechallenged on day 71 with double the number of 4T1 cells, and all of them remained alive and appeared healthy. Upon sacrifice on day 140, the lungs were found free of visible surface nodules. Furthermore, H&E staining was performed on lung sections of these mice, and the lung tissue appeared free of metastasis (Fig. 2B). The 100% survival rate and tumor-free status in B7x$^{-/-}$ mice after 4T1 rechallenge confirmed a memory response against 4T1.

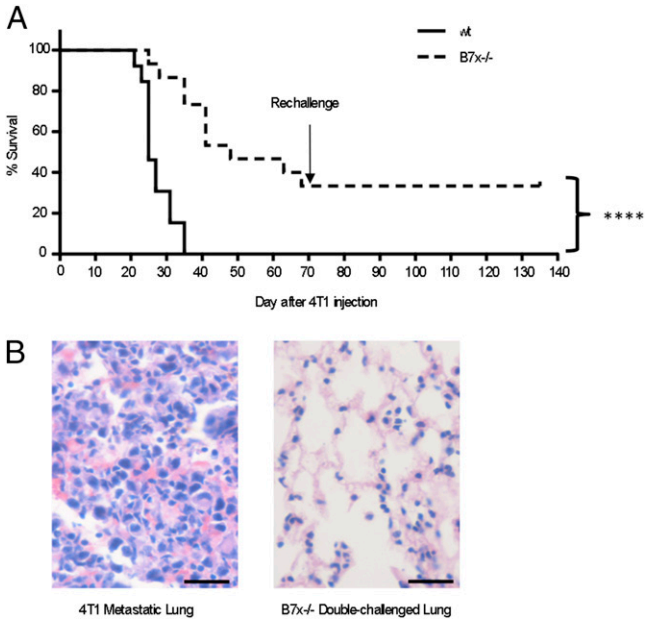


**FIGURE 2.** B7x knockout mice can survive 4T1 and 4T1 rechallenge. (**A**) Survival of mice injected with 4T1 cells in the tail vein ($n$ = 13–15). Data are representative of two separate experiments. At 71 d postinjection, remaining mice were rechallenged with double the number of 4T1 cells. (**B**) H&E staining of lung sections of the double-challenged mice at day 140 and other 4T1-injected mice. Lung tissue bearing 4T1 metastasis (*left panel*). Representative lung tissue from the double-challenged B7x$^{-/-}$ mice (*right panel*). Scale bar, 25 μm. ****$p < 0.0001$.

*B7x knockout mice generate higher T cell cytokine responses*

The 4T1 metastasis and survival results revealed that tissue B7x deficiency resulted in protection from malignancy with the ability to generate immune memory. To investigate the protective mechanism, we isolated the immune cell infiltrate from the lungs of wt and B7x$^{-/-}$ mice injected with 4T1 i.v. and analyzed the cell populations by flow cytometry. Surprisingly, we did not find a significant difference in the total number of T cells, B cells, NK cells, or DCs (Fig. 3A). However, a functional difference between T cells in the lungs of B7x$^{-/-}$ and wt mice was observed in the enhanced ability of T cells derived from the lungs of B7x$^{-/-}$ mice to produce inflammatory cytokines IFN-γ and TNF-α in response to PMA/ionomycin stimulation (Fig. 3B, 3C). We further tested whether T cells from lungs of B7x$^{-/-}$ mice had an increased ability to generate a tumor-specific response. DCs were generated from wt bone marrow, loaded with 4T1 lysate, and incubated with total immune cells isolated from lungs of 4T1-injected wt and B7x$^{-/-}$ mice. We found that the CD8 T cells from B7x$^{-/-}$ mice produced significantly more IFN-γ in response to 4T1 lysate–loaded DCs than did those from wt mice (Fig. 3D, 3E). Thus, T cells from 4T1-injected B7x$^{-/-}$ mice appeared to be more functionally competent and tumor responsive than did those from 4T1-injected wt mice, suggesting that T cells from wt, but not B7x$^{-/-}$, lungs may have been in a suppressed state.

*B7x knockout mice have a lower immunosuppressive cell infiltrate*

Suppression of T cells in the context of cancer often results from tumor recruitment of immunosuppressive cells and factors. Therefore, we investigated the immunosuppressive cell infiltrates in the lungs of wt and B7x$^{-/-}$ mice. We found that wt mice had a significantly higher percentage and total number of Foxp3$^{+}$CD4$^{+}$ Tregs in the lungs than did B7x$^{-/-}$ mice (Fig. 4A, 4B). F4/80$^{+}$ macrophages were also increased in number in lung, as well as spleen, of wt mice (Fig. 4B). Most striking, however, was the huge population of CD11b$^{+}$Ly6G$^{+}$ cells found infiltrating both lung and spleen of metastatic mice (Fig. 4B, 4C). It was reported that implanted 4T1 tumors induce a leukemoid reaction, resulting in myeloid cell overproduction in bone marrow and high levels of granulocytic cells in peripheral blood and spleen (33). In the tail vein 4T1 model, we too observed a large increase in the percentage and total number of these myeloid cells in spleen, as well as in lung, of wt and B7x$^{-/-}$ mice. However, the percentage and total number were significantly reduced in B7x$^{-/-}$ mice. Tumor-associated cells double positive for CD11b and Ly6G are often referred to as myeloid-derived suppressor cells (MDSCs) (34). Both Tregs and MDSCs are known to suppress T cell responses. The reduction in both of these cell populations in B7x$^{-/-}$ mice afforded them a significantly higher ratio of effector CD4 and CD8 T cells to the Tregs and, presumably, suppressive MDSCs (Fig. 4D). These results suggest that the presence of B7x may have resulted in indirect inhibitory effects on T cells through suppressor cell populations.

*Metastatic lung–infiltrating CD11b$^{+}$Ly6G$^{+}$ cells are GR1$^{hi}$ TANs*

Because of the overwhelming CD11b$^{+}$Ly6G$^{+}$ MDSC infiltrate into the lung and spleen of 4T1-injected mice and the significant re-

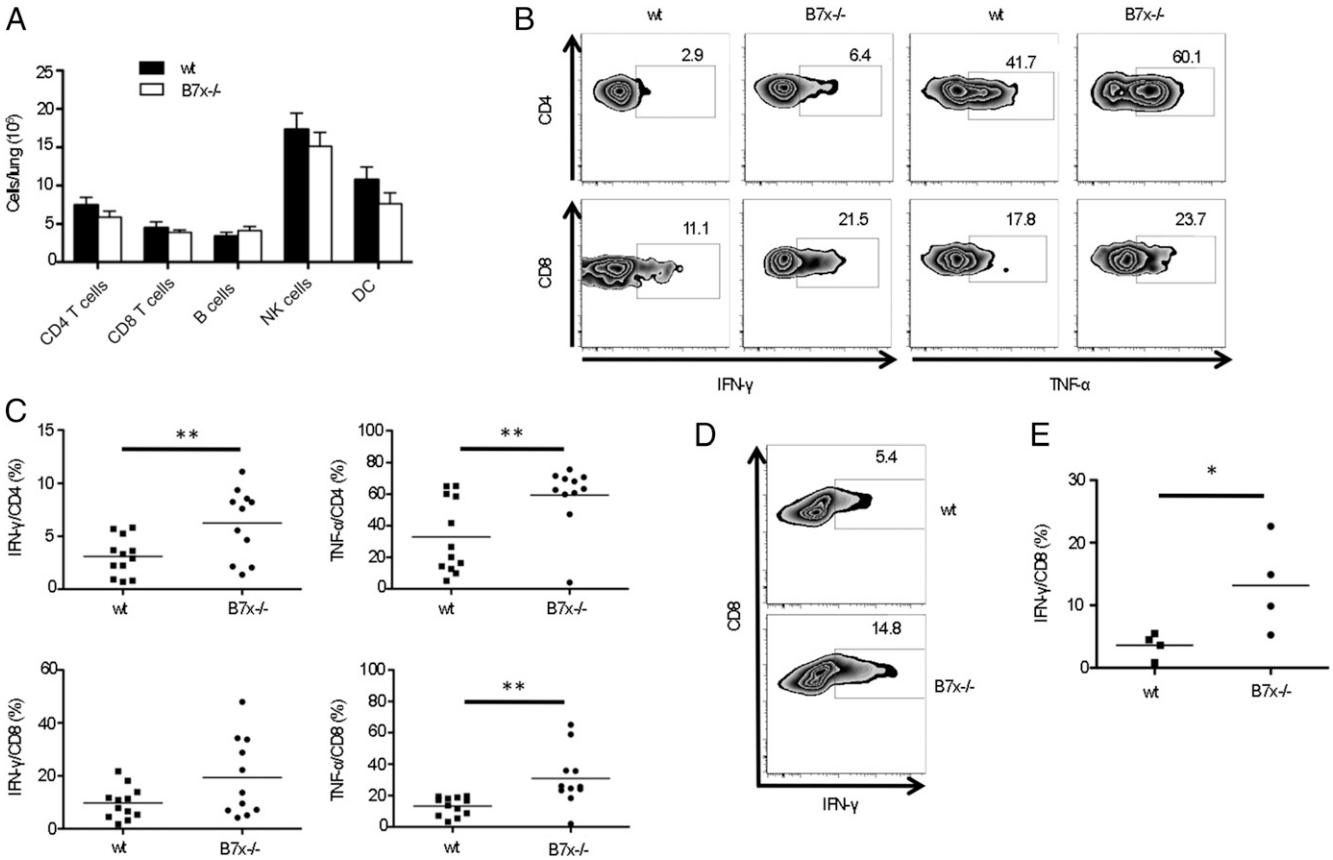


**FIGURE 3.** Analysis of lung immune cell infiltrate reveals higher cytokine responses to general and tumor-specific stimulation by T cells from knockout mice. (**A**) Numbers of immune effector cells infiltrating lungs at 17–18 d after 4T1 injection. Data are pooled from two to five experiments ($n = 8–22$). (**B** and **C**) PMA/ionomycin-stimulated T cells from lungs of 4T1-injected mice were analyzed for cytokine production. Percentages of IFN-γ$^{+}$ or TNF-α$^{+}$ cells are shown in representative FACS plots (B) and pooled from three independent experiments; each symbol represents an individual mouse (C) ($n = 11–12$). CD8 T cell cytokine response after stimulation with 4T1 lysate–loaded DCs shown as representative FACS plots (**D**) and percentages of IFN-γ$^{+}$ cells (**E**) ($n = 4$). *$p < 0.05$, **$p < 0.01$.

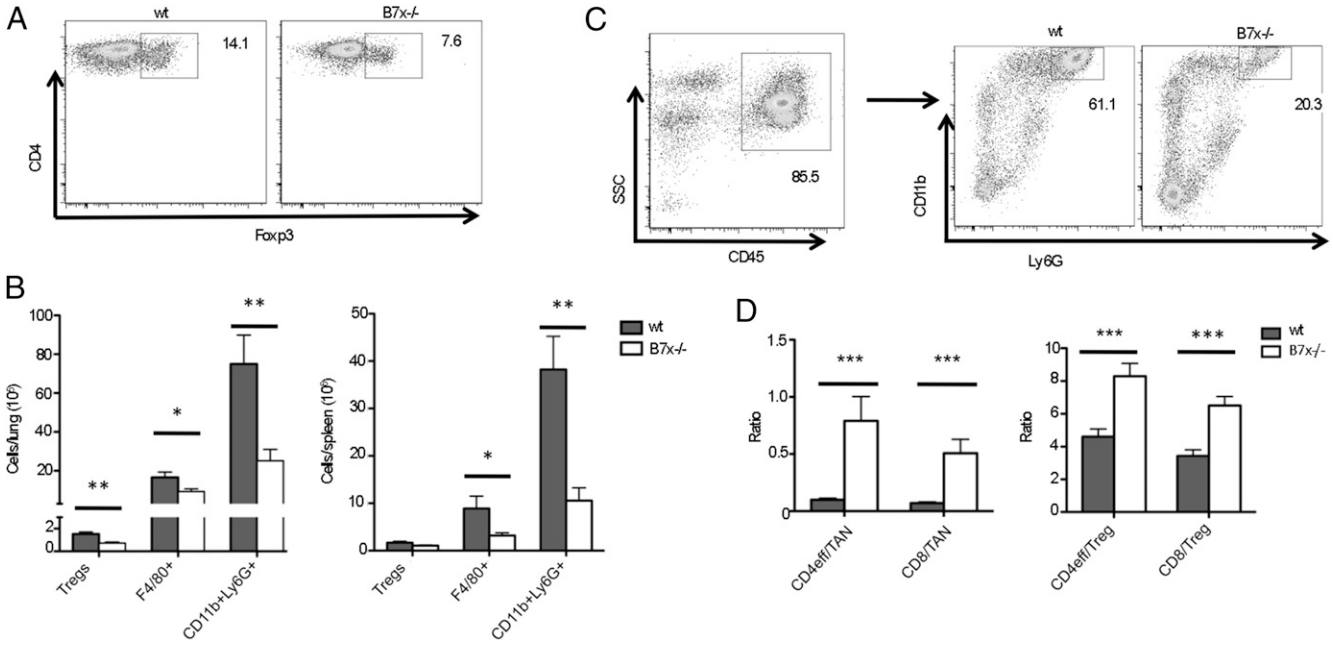


**FIGURE 4.** B7x knockout mice have fewer suppressive cells and a higher ratio of effector/suppressor cells. Cell suspensions from lungs and spleens of day-17–18 4T1-injected wt and B7x$^{-/-}$ mice were stained with lineage markers. (**A**) Representative FACS plots of permeabilized CD4 cells stained for Foxp3. (**B**) Cell type numbers were determined by flow cytometry. Data are pooled from four or five independent experiments ($n$ = 16–22, lungs, *left panel*) and two to four experiments ($n$ = 8–10, spleens, *right panel*). (**C**) Representative FACS plots of CD11b$^{+}$Ly6G$^{+}$ cells among total CD45$^{+}$ cells in wt and B7x$^{-/-}$ lungs. (**D**) The ratios of Foxp3$^{-}$CD4$^{+}$ (CD4$_{eff}$) and CD8 T cells to CD11b$^{+}$Ly6G$^{+}$ (TAN) cells (*left panel*) and CD4$_{eff}$ and CD8 T cells to Foxp3$^{+}$ CD4$^{+}$ (Treg) cells (*right panel*) were calculated within each lung sample. Results are pooled from four independent experiments ($n$ = 16–18). *$p < 0.05$, **$p < 0.01$, ***$p < 0.001$.

duction in B7x$^{-/-}$ mice, we took a closer look at the phenotype and function of these cells. MDSCs have been reported as a heterogeneous group of cells that can include monocytic and/or granulocytic cells at various stages of maturity. The Ly6G marker on MDSCs can help to identify the MDSC subtype, depending on the Ab clone. The Ly6G Ab clone RB6-8C5, also called GR1, recognizes the Ly6C epitope on monocytic cells, as well as a granulocytic epitope called Ly6G (35). In contrast, the Ly6G Ab clone 1A8 only recognizes the granulocyte-specific Ly6G epitope (36). We used the 1A8 clone in the experiments evaluating the percentage and number of CD11b$^{+}$Ly6G$^{+}$ cells infiltrating the lung and spleen, as well as in all subsequent experiments. We found, using flow cytometry, that the cells expressing CD11b and Ly6G clone 1A8 were GR1$^{hi}$ and Ly6C$^{lo/int}$ and that the overwhelming majority of myeloid cells (CD11b$^{+}$) and CD11b$^{+}$GR1$^{+}$ cells in this model were Ly6G$^{hi}$ granulocytes (Fig. 5A).

To further identify these cells morphologically, we separated Ly6G$^{hi}$ cells from wt and B7x$^{-/-}$ 4T1-metastatic lungs using FACS, adhered them to slides using Cytospin, and stained them with hematoxylin. We found that the sorted cells showed the characteristic morphology of neutrophils, with ring-shaped and/or segmented nuclei (Fig. 5B), confirming that the myeloid cell influx in this model was predominantly neutrophilic. Therefore, our results suggest that host B7x affected TANs in pulmonary metastasis.

### *Neutrophils isolated from tumor-bearing lungs suppress T cell proliferation*

MDSCs were reported to inhibit T cell responses in various models (37–39). Therefore, we tested whether the neutrophilic MDSCs, or TANs, in the 4T1-metastatic lungs were indeed capable of suppressing T cell responses. We designed an in vitro coculture system, stimulating CFSE-labeled T cells from naive wt spleen with plate-bound anti-CD3 in the presence of neutrophils purified from either naive bone marrow (control) or metastatic lung (TANs) from wt or B7x$^{-/-}$ mice. We found that TANs from metastatic lungs, but not naive bone marrow neutrophils, suppressed T cell proliferation, as observed by CFSE dilution, when plated at a neutrophil/T cell ratio ≥1:1 (Fig. 6A). After 4 d in culture with stimulation, CFSE dilution revealed that ~90% or more of T cells plated alone or with bone marrow–naive neutrophils were in divisions 1–7, whereas only 30–70% of T cells cocultured with TANs were in division; in many cases, the majority of T cells cocultured with TANs had not divided at all. Correspondingly, the proliferation index of T cells cultured with lung TANs was significantly lower in both CD4 and CD8 T cells compared with those cultured with control neutrophils (Fig. 6B). Surprisingly, TANs from B7x$^{-/-}$ mice, as well as wt mice, could suppress T cell proliferation, suggesting that the TANs infiltrating both wt and B7x$^{-/-}$ mice were suppressive and differed in number (Fig. 4C) but not in function (Fig. 6B).

### *B7x-Ig strongly binds TANs*

The ability of neutrophils from 4T1-metastatic lungs to suppress the proliferation of T cells suggested a mechanism by which T cell responses against growing metastases in the lung were kept limited. We next investigated the role of B7x expression in lung tissue in this process. We asked whether B7x was directly involved in regulating immune cell responses through expression on the surface of immune cells or through interactions with these cells. B7x protein expression has been reported inconsistently, with some reports showing that B7x is induced on some immune cells (23, 24) and others reporting that immune cells are B7x negative (26, 27, 40). We found that all CD45$^{+}$ immune cells infiltrating 4T1-metastatic lungs of wt mice, including APCs and neutrophils, were negative for B7x expression (Fig. 7A). Therefore, we turned our attention to immune cells that could bind B7x. Because the B7x receptor is unknown, we looked for cells that might express the B7x receptor using an engineered fusion protein consisting of the extracellular domain of B7x and the Fc portion of human IgG1

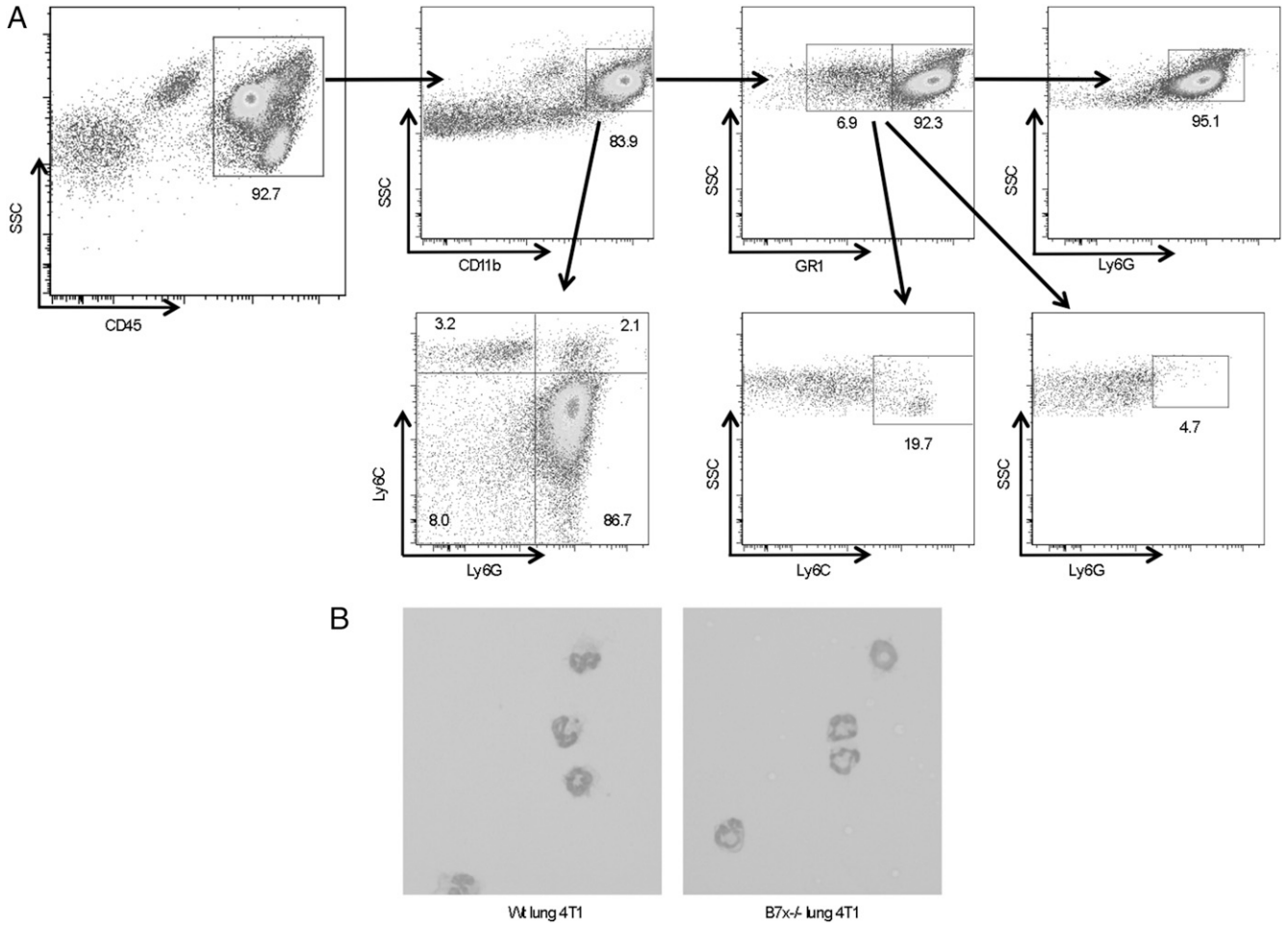


**FIGURE 5.** $CD11b^{+}Ly6G^{+}$ cells infiltrating metastatic wt and $B7x^{-/-}$ lungs are $GR1^{hi}$ morphologically mature neutrophils. (**A**) Metastatic lung cell suspensions were stained with lineage markers. Shown is a representative wt lung sample gated on CD45 and analyzed for CD11b, GR1, Ly6G, and Ly6C expression. (**B**) $Ly6G^{hi}$ cells sorted from lungs of 4T1-injected wt and $B7x^{-/-}$ mice were stained with hematoxylin following Cytospin centrifugation. Representative images are shown (original magnification ×40).

(22), which could be detected with an anti-human IgG fluorophore–conjugated Ab. To our surprise, we found that this B7x-Ig fusion protein bound very strongly to neutrophils isolated from 4T1-metastatic lungs (Fig. 7B), suggesting that neutrophils express a receptor for B7x. The B7x-Ig also could slightly bind naive neutrophils, from lungs of wt and $B7x^{-/-}$ mice (Fig. 7C) and two human cell lines of neutrophilic lineage HL60 and AP-60, but not from other human cell lines, such as Jurkat, Raji, and HeLa cells (Fig. 7D). However, the strongest binding was observed in neutrophils from the lungs, spleen, and blood of mice whose lungs were highly metastatic, suggesting that the neutrophils in these mice upregulate their putative B7x receptor in response to growing 4T1 metastases or that they may be a different type of neutrophil that has a receptor with a stronger affinity for B7x . These findings suggest an unexpected mechanism of immunosuppression in metastatic mice, whereby B7x on local lung tissue binds TANs, which, together with Tregs, suppress T cells. Perhaps together with inhibition of T cells by direct binding of lung B7x, TAN-induced suppression results in reduced antitumor immunity and increased metastasis.

## Discussion

This study revealed that host B7x promotes metastatic tumor growth in an in vivo cancer model. Although many clinical studies showed B7x overexpression in human cancers and a strong correlation with metastasis, cancer recurrence, and/or cancer-related death (6–17), it was unclear whether B7x was causative or merely correlative. In this study, B7x deficiency in mice resulted in significant protection from lung metastases and increased survival in the 4T1 tumor model.

Using 4T1 in an experimental metastasis model highlighted the effect of lung B7x specifically on the growth and establishment of metastasized cells. Tumor cells were deposited directly into the circulation, bypassing primary tumor and the early stages of metastasis. Because lung is the first organ receiving blood supply from the circulation, tumor cells in the circulation preferentially extravasate there and, if the conditions are right, establish metastases (41). Therefore, this model did not allow for exploration of the effect of B7x on most steps of the metastatic cascade, but it did directly evaluate the connection between the presence of host B7x and growth of metastatic colonies from cells that have successfully metastasized to lung tissue. Because B7x is present in the lungs of wt mice, but not in $B7x^{-/-}$ mice, the highly increased growth of lung metastases in wt mice supported the notion that B7x was a factor in the lungs promoting metastatic growth.

It was hypothesized that B7x upregulated on cancer cells protects them from tumor-infiltrating CTLs by binding and inhibiting them, thus enabling tumor progression (22, 42, 43). We found that the T cells in $B7x^{-/-}$ lungs appeared to be more functional and tumor responsive than were those in wt mice, because they produced

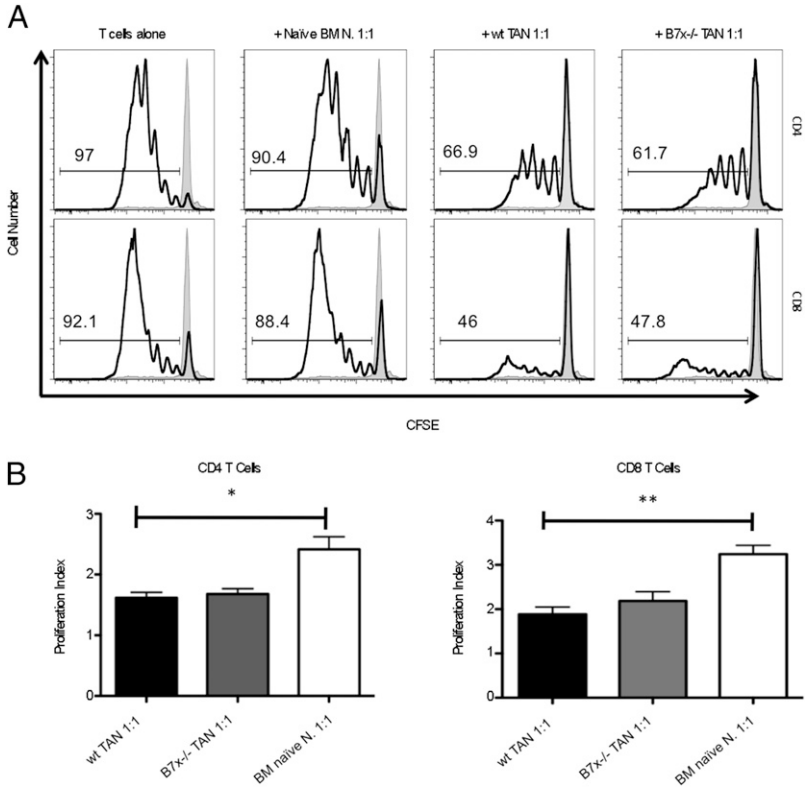


**FIGURE 6.** Neutrophils isolated from tumor-bearing lungs suppress T cell proliferation. A total of $10^5$ CFSE-labeled T cells from naive spleen was stimulated with plate-bound anti-CD3 alone or in the presence of $10^5$ neutrophils purified from naive bone marrow or from 4T1-metastatic wt or B7x$^{-/-}$ lungs. After 4 d, cells were stained with CD4, CD8, and Live/Dead marker and acquired by flow cytometry. (**A**) Representative FACS plots show CFSE dilution among live CD4-gated and CD8-gated stimulated (open graphs) and unstimulated control (shaded graphs) T cells. (**B**) Proliferative index of CD4 and CD8 T cells cocultured with control or wt TANs was calculated using FlowJo software. Results are pooled from two or three independent experiments ($n$ = 3–10). *$p < 0.05$, **$p < 0.01$.

more inflammatory cytokines in response to general and tumor-specific stimulation. One explanation for this is that B7x expressed on lung tissue cells in wt mice acted directly on T cells by binding them and inhibiting their function. Because T cells were less functional in wt mice, tumors grew and recruited more Tregs and TANs, which had further suppressive effects on T cells. This cycle

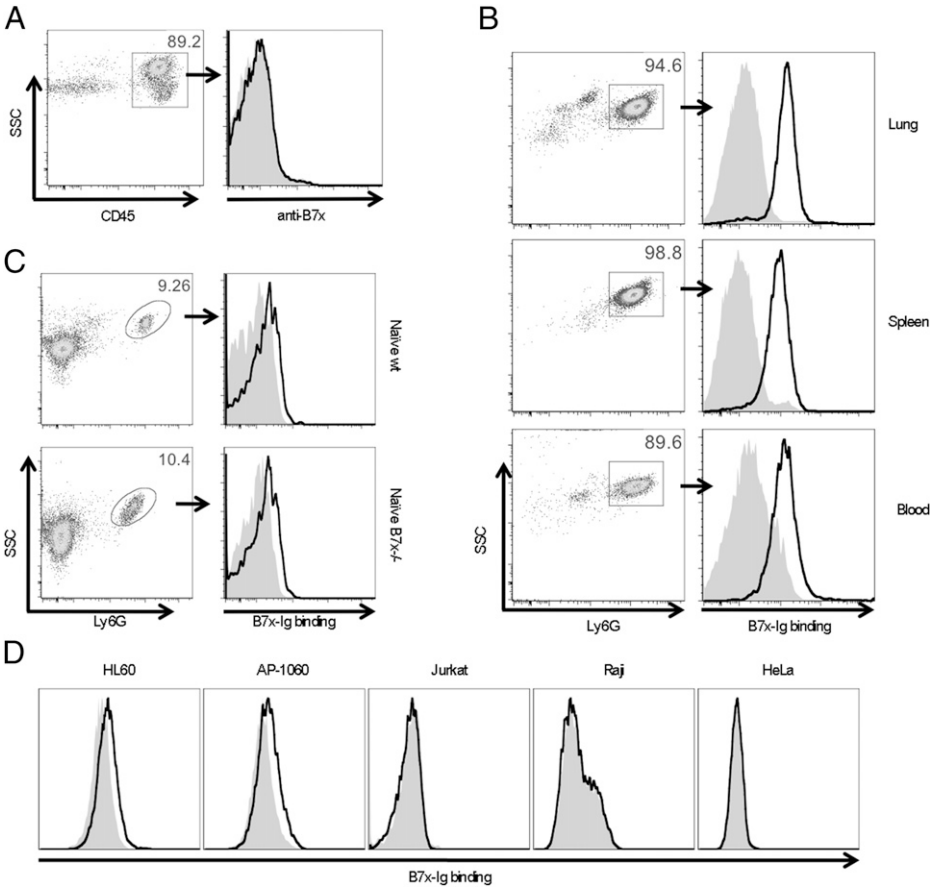


**FIGURE 7.** TANs strongly bind B7x. (**A**) Single-cell suspensions from lungs of wt 4T1-injected mice were stained with CD45 and anti-B7x (open graphs) or isotype control (shaded graphs). Ly6G$^+$ cells isolated from lung and spleen and RBC-depleted blood cells from 4T1-injected wt mice (**B**) and naive wt and B7x$^{-/-}$ lung cell suspensions (**C**) were incubated with B7x-Ig (open graphs) or control Hu-IgG (shaded graphs), followed by staining with Ly6G and Ab recognizing the Ig portion of both fusion proteins (anti–Hu-IgG). (**D**) Cells were incubated with B7x-Ig (open graphs) or Hu-IgG (shaded graphs) and stained with anti–Hu-IgG. Graphs in (A–C) are representative of two to five separate experiments. Staining of HL-60 was repeated three times with similar results.

was reduced in B7x$^{-/-}$ mice because their T cells remained functional and were more capable of controlling tumor growth.

A second explanation is that the TANs recruited into tumor-bearing lungs had a more dominant role in inhibiting T cell function, and this was enhanced by the presence of B7x. An association between B7x expression and neutrophils was reported in the context of infection. In one study, B7x$^{-/-}$ mice infected i.p. with *Listeria monocytogenes* had an increased neutrophil response compared with wt mice (44). In contrast, B7x$^{-/-}$ mice intranasally infected with *Streptococcus pneumoniae* had a reduced neutrophil response (25). Although neither study describes the nature of the link between B7x and neutrophils, a connection between B7x and neutrophil density is nonetheless highlighted. In the current study, we found that TANs were highly increased in the lungs of wt mice, corresponding to the extent of lung metastasis. We found that these TANs were capable of suppressing T cell proliferation in vitro, suggesting that they functioned to reduce antitumor immune responses in the lungs, thereby supporting metastatic growth. These results are consistent with other studies demonstrating various protumor effects of TANs (45), including a recent study in which depletion of TANS with anti-Ly6G increased antitumor immunity in an experimental lung metastasis model (46). Furthermore, an important, unexpected finding in this study was that TANs could bind B7x. To our knowledge, this is the first study revealing B7x binding to cells other than activated T cells. We found that B7x-Ig could slightly bind naive neutrophils from lung and strongly bind TANs from highly metastatic lungs. This suggested that TANs upregulated their putative B7x receptor in response to growing metastases. Furthermore, it suggested that B7x had an important effect on TANs, which, in turn, could suppress T cell responses against tumor. Therefore, it is possible that the binding of B7x expressed on lung or other tissue cells to TANs led to enhanced TAN density and/or function and, thereby, resulted in increased metastatic growth in wt mice. Future work is necessary to distinguish whether host tissue–expressed B7x primarily causes immunosuppression through direct inhibition of T cells, through effects on TANs resulting in indirect inhibition of T cells, or through a combination of both mechanisms.

We identified the CD11b$^{+}$Ly6G$^{+}$ cells infiltrating 4T1-metastatic lungs as TANs on the basis of their expression of the specific granulocytic Ly6G marker, neutrophil morphology, and infiltration into tumor. Whether and how TANs are distinct from granulocytic MDSCs is under investigation (47, 48). However, we did not distinguish between these terms and consider our findings a contribution to MDSC research, in general, and the granulocytic MDSC and TAN fields, in particular. Although there are extensive reports showing suppression of T cells by monocytic MDSCs or MDSCs consisting of mixed monocytic and granulocytic subsets, there is less definitive evidence regarding the suppressive capabilities of granulocytic MDSCs or TANs (48). Furthermore, most published reports on MDSCs focused on MDSC suppression only of CD8 T cells or only under Ag-specific conditions (34, 37, 39, 49, 50). In contrast, in the tail vein 4T1 model, we revealed TAN suppression of proliferation of both CD4 and CD8 T cells in response to general anti-CD3 stimulation. This unusual result may be due to the fact that we used CD11b$^{+}$Ly6G$^{+}$ cells from tumor-bearing lungs as opposed to splenic MDSCs, which are used in many studies. Tumor MDSCs were reported to be more suppressive than splenic MDSCs (51).

Although the binding of B7x-Ig to TANs provided an important link between TAN accumulation and the presence of B7x, the functional relationship between B7x and TANs was difficult to decipher. Using in vitro systems, we failed to detect any effect of B7x-Ig on TAN survival or production of suppressive factors, such as reactive oxygen species, arginase, or NO (data not shown). Furthermore, TANs from B7x$^{-/-}$ mice could also suppress T cells in vitro if the TANs were isolated from mice with metastatic lungs, which happened in a percentage of B7x$^{-/-}$ mice. Therefore, the most salient difference between TANs in wt and B7x$^{-/-}$ mice was their number. The reduction in both TANs and Tregs in B7x$^{-/-}$ mice provided them with a far more favorable effector/suppressor ratio than in wt mice, which could explain the enhanced T cell responses to ex vivo stimulation, as well as the reduced 4T1 metastasis and improved survival, in B7x$^{-/-}$ mice. Further study is necessary to clarify the exact functional relationship between B7x expressed in nontumor tissue, MDSCs, effector T cells, and Tregs, as well as to identify the receptor for B7x both on T cells and myeloid cells.

## Acknowledgments

We thank Fred Miller (Wayne State University School of Medicine, Detroit, MI) for providing 4T1 cells, Robert Gallagher (Montefiore Medical Center, Bronx, NY) for providing HL-60 and AP-1060 cell lines and protocols, and James Allison (Memorial Sloan-Kettering Cancer Center, New York, NY) for support at the start of this project. We also thank the Albert Einstein College of Medicine Flow Cytometry Core for assistance.

## Disclosures

The authors have no financial conflicts of interest.

## References

1. Chambers, A. F., A. C. Groom, and I. C. MacDonald. 2002. Dissemination and growth of cancer cells in metastatic sites. *Nat. Rev. Cancer* 2: 563–572.
2. Joyce, J. A., and J. W. Pollard. 2009. Microenvironmental regulation of metastasis. *Nat. Rev. Cancer* 9: 239–252.
3. de Souza, A. P., and C. Bonorino. 2009. Tumor immunosuppressive environment: effects on tumor-specific and nontumor antigen immune responses. *Expert Rev. Anticancer Ther.* 9: 1317–1332.
4. Dunn, G. P., L. J. Old, and R. D. Schreiber. 2004. The immunobiology of cancer immunosurveillance and immunoediting. *Immunity* 21: 137–148.
5. Rosenberg, S. A. 2008. Overcoming obstacles to the effective immunotherapy of human cancer. *Proc. Natl. Acad. Sci. USA* 105: 12643–12644.
6. Krambeck, A. E., R. H. Thompson, H. Dong, C. M. Lohse, E. S. Park, S. M. Kuntz, B. C. Leibovich, M. L. Blute, J. C. Cheville, and E. D. Kwon. 2006. B7-H4 expression in renal cell carcinoma and tumor vasculature: associations with cancer progression and survival. *Proc. Natl. Acad. Sci. USA* 103: 10391–10396.
7. Mugler, K. C., M. Singh, B. Tringler, K. C. Torkko, W. Liu, J. Papkoff, and K. R. Shroyer. 2007. B7-h4 expression in a range of breast pathology: correlation with tumor T-cell infiltration. *Appl. Immunohistochem. Mol. Morphol.* 15: 363–370.
8. Salceda, S., T. Tang, M. Kmet, A. Munteanu, M. Ghosh, R. Macina, W. Liu, G. Pilkington, and J. Papkoff. 2005. The immunomodulatory protein B7-H4 is overexpressed in breast and ovarian cancers and promotes epithelial cell transformation. *Exp. Cell Res.* 306: 128–141.
9. Simon, I., S. Zhuo, L. Corral, E. P. Diamandis, M. J. Sarno, R. L. Wolfert, and N. W. Kim. 2006. B7-h4 is a novel membrane-bound protein and a candidate serum and tissue biomarker for ovarian cancer. *Cancer Res.* 66: 1570–1575.
10. Sun, Y., Y. Wang, J. Zhao, M. Gu, R. Giscombe, A. K. Lefvert, and X. Wang. 2006. B7-H3 and B7-H4 expression in non-small-cell lung cancer. *Lung Cancer* 53: 143–151.
11. Tringler, B., W. Liu, L. Corral, K. C. Torkko, T. Enomoto, S. Davidson, M. S. Lucia, D. E. Heinz, J. Papkoff, and K. R. Shroyer. 2006. B7-H4 overexpression in ovarian tumors. *Gynecol. Oncol.* 100: 44–52.
12. Tringler, B., S. Zhuo, G. Pilkington, K. C. Torkko, M. Singh, M. S. Lucia, D. E. Heinz, J. Papkoff, and K. R. Shroyer. 2005. B7-h4 is highly expressed in ductal and lobular breast cancer. *Clin. Cancer Res.* 11: 1842–1848.
13. Yao, Y., X. Wang, K. Jin, J. Zhu, Y. Wang, S. Xiong, Y. Mao, and L. Zhou. 2008. B7-H4 is preferentially expressed in non-dividing brain tumor cells and in a subset of brain tumor stem-like cells. *J. Neurooncol.* 89: 121–129.
14. Thompson, R. H., X. Zang, C. M. Lohse, B. C. Leibovich, S. F. Slovin, V. E. Reuter, J. C. Cheville, M. L. Blute, P. Russo, E. D. Kwon, and J. P. Allison. 2008. Serum-soluble B7x is elevated in renal cell carcinoma patients and is associated with advanced stage. *Cancer Res.* 68: 6054–6058.
15. Zang, X., R. H. Thompson, H. A. Al-Ahmadie, A. M. Serio, V. E. Reuter, J. A. Eastham, P. T. Scardino, P. Sharma, and J. P. Allison. 2007. B7-H3 and B7x are highly expressed in human prostate cancer and associated with disease spread and poor outcome. *Proc. Natl. Acad. Sci. USA* 104: 19458–19463.
16. Zang, X., P. S. Sullivan, R. A. Soslow, R. Waitz, V. E. Reuter, A. Wilton, H. T. Thaler, M. Arul, S. F. Slovin, J. Wei, et al. 2010. Tumor associated endothelial expression of B7-H3 predicts survival in ovarian carcinomas. *Mod. Pathol.* 23: 1104–1112.

17. Jiang, J., Y. Zhu, C. Wu, Y. Shen, W. Wei, L. Chen, X. Zheng, J. Sun, B. Lu, and X. Zhang. 2010. Tumor expression of B7-H4 predicts poor survival of patients suffering from gastric cancer. *Cancer Immunol. Immunother.* 59: 1707–1714.
18. Chen, L. J., J. Sun, H. Y. Wu, S. M. Zhou, Y. Tan, M. Tan, B. E. Shan, B. F. Lu, and X. G. Zhang. 2011. B7-H4 expression associates with cancer progression and predicts patient's survival in human esophageal squamous cell carcinoma. *Cancer Immunol. Immunother.* 60: 1047–1055.
19. Arigami, T., Y. Uenosono, M. Hirata, T. Hagihara, S. Yanagita, S. Ishigami, and S. Natsugoe. 2010. Expression of B7-H4 in blood of patients with gastric cancer predicts tumor progression and prognosis. *J. Surg. Oncol.* 102: 748–752.
20. Arigami, T., Y. Uenosono, S. Ishigami, T. Hagihara, N. Haraguchi, and S. Natsugoe. 2011. Clinical significance of the B7-H4 coregulatory molecule as a novel prognostic marker in gastric cancer. *World J. Surg.* 35: 2051–2057.
21. Miyatake, T., B. Tringler, W. Liu, S. H. Liu, J. Papkoff, T. Enomoto, K. C. Torkko, D. L. Dehn, A. Swisher, and K. R. Shroyer. 2007. B7-H4 (DD-O110) is overexpressed in high risk uterine endometrioid adenocarcinomas and inversely correlated with tumor T-cell infiltration. *Gynecol. Oncol.* 106: 119–127.
22. Zang, X., P. Loke, J. Kim, K. Murphy, R. Waitz, and J. P. Allison. 2003. B7x: a widely expressed B7 family member that inhibits T cell activation. *Proc. Natl. Acad. Sci. USA* 100: 10388–10392.
23. Sica, G. L., I. H. Choi, G. Zhu, K. Tamada, S. D. Wang, H. Tamura, A. I. Chapoval, D. B. Flies, J. Bajorath, and L. Chen. 2003. B7-H4, a molecule of the B7 family, negatively regulates T cell immunity. *Immunity* 18: 849–861.
24. Prasad, D. V., S. Richards, X. M. Mai, and C. Dong. 2003. B7S1, a novel B7 family member that negatively regulates T cell activation. *Immunity* 18: 863–873.
25. Hofmeyer, K. A., L. Scandiuzzi, K. Ghosh, L. A. Pirofski, and X. Zang. 2012. Tissue-expressed B7x affects the immune response to and outcome of lethal pulmonary infection. *J. Immunol.* 189: 3054–3063.
26. Wei, J., P. Loke, X. Zang, and J. P. Allison. 2011. Tissue-specific expression of B7x protects from CD4 T cell-mediated autoimmunity. *J. Exp. Med.* 208: 1683–1694.
27. Lee, J. S., L. Scandiuzzi, A. Ray, J. Wei, K. A. Hofmeyer, Y. M. Abadi, P. Loke, J. Lin, J. Yuan, D. V. Serreze, et al. 2012. B7x in the periphery abrogates pancreas-specific damage mediated by self-reactive CD8 T cells. *J. Immunol.* 189: 4165–4174.
28. Chen, Y., C. Yang, Z. Xie, L. Zou, Z. Ruan, X. Zhang, Y. Tang, L. Fei, Z. Jia, and Y. Wu. 2006. Expression of the novel co-stimulatory molecule B7-H4 by renal tubular epithelial cells. *Kidney Int.* 70: 2092–2099.
29. Aslakson, C. J., and F. R. Miller. 1992. Selective events in the metastatic process defined by analysis of the sequential dissemination of subpopulations of a mouse mammary tumor. *Cancer Res.* 52: 1399–1405.
30. Sun, Y., S. H. Kim, D. C. Zhou, W. Ding, E. Paietta, F. Guidez, A. Zelent, K. H. Ramesh, L. Cannizzaro, R. P. Warrell, and R. E. Gallagher. 2004. Acute promyelocytic leukemia cell line AP-1060 established as a cytokine-dependent culture from a patient clinically resistant to all-trans retinoic acid and arsenic trioxide. *Leukemia* 18: 1258–1269.
31. Fan, T. M. 2007. Murine and canine models of appendicular osteosarcoma. *Curr. Protoc. Pharmacol*. Chapter 14: Unit 14.1.
32. Roederer, M. 2011. Interpretation of cellular proliferation data: avoid the panglossian. *Cytometry A* 79: 95–101.
33. DuPre', S. A., and K. W. Hunter, Jr. 2007. Murine mammary carcinoma 4T1 induces a leukemoid reaction with splenomegaly: association with tumor-derived growth factors. *Exp. Mol. Pathol.* 82: 12–24.
34. Gabrilovich, D. I., and S. Nagaraj. 2009. Myeloid-derived suppressor cells as regulators of the immune system. *Nat. Rev. Immunol.* 9: 162–174.
35. Peranzoni, E., S. Zilio, I. Marigo, L. Dolcetti, P. Zanovello, S. Mandruzzato, and V. Bronte. 2010. Myeloid-derived suppressor cell heterogeneity and subset definition. *Curr. Opin. Immunol.* 22: 238–244.
36. Daley, J. M., A. A. Thomay, M. D. Connolly, J. S. Reichner, and J. E. Albina. 2008. Use of Ly6G-specific monoclonal antibody to deplete neutrophils in mice. *J. Leukoc. Biol.* 83: 64–70.
37. Youn, J. I., S. Nagaraj, M. Collazo, and D. I. Gabrilovich. 2008. Subsets of myeloid-derived suppressor cells in tumor-bearing mice. *J. Immunol.* 181: 5791–5802.
38. Corzo, C. A., M. J. Cotter, P. Cheng, F. Cheng, S. Kusmartsev, E. Sotomayor, T. Padhya, T. V. McCaffrey, J. C. McCaffrey, and D. I. Gabrilovich. 2009. Mechanism regulating reactive oxygen species in tumor-induced myeloid-derived suppressor cells. *J. Immunol.* 182: 5693–5701.
39. Movahedi, K., M. Guilliams, J. Van den Bossche, R. Van den Bergh, C. Gysemans, A. Beschin, P. De Baetselier, and J. A. Van Ginderachter. 2008. Identification of discrete tumor-induced myeloid-derived suppressor cell subpopulations with distinct T cell-suppressive activity. *Blood* 111: 4233–4244.
40. Kamimura, Y., H. Kobori, J. Piao, M. Hashiguchi, K. Matsumoto, S. Hirose, and M. Azuma. 2009. Possible involvement of soluble B7-H4 in T cell-mediated inflammatory immune responses. *Biochem. Biophys. Res. Commun.* 389: 349–353.
41. Elkin, M., and I. Vlodavsky. 2001. Tail vein assay of cancer metastasis. *Curr. Protoc. Cell Biol.* Chapter 19: Unit 19.12.
42. Zang, X., and J. P. Allison. 2007. The B7 family and cancer therapy: costimulation and coinhibition. *Clin. Cancer Res.* 13: 5271–5279.
43. Barach, Y. S., J. S. Lee, and X. Zang. 2010. T cell coinhibition in prostate cancer: new immune evasion pathways and emerging therapeutics. *Trends Mol. Med.* 17: 47–55.
44. Zhu, G., M. M. Augustine, T. Azuma, L. Luo, S. Yao, S. Anand, A. C. Rietz, J. Huang, H. Xu, A. S. Flies, et al. 2009. B7-H4-deficient mice display augmented neutrophil-mediated innate immunity. *Blood* 113: 1759–1767.
45. Fridlender, Z. G., J. Sun, S. Kim, V. Kapoor, G. Cheng, L. Ling, G. S. Worthen, and S. M. Albelda. 2009. Polarization of tumor-associated neutrophil phenotype by TGF-beta: "N1" versus "N2" TAN. *Cancer Cell* 16: 183–194.
46. Srivastava, M. K., L. Zhu, M. Harris-White, U. Kar, M. Huang, M. F. Johnson, J. M. Lee, D. Elashoff, R. Strieter, S. Dubinett, and S. Sharma. 2012. Myeloid suppressor cell depletion augments antitumor activity in lung cancer. *PLoS ONE* 7: e40677.
47. Youn, J. I., M. Collazo, I. N. Shalova, S. K. Biswas, and D. I. Gabrilovich. 2012. Characterization of the nature of granulocytic myeloid-derived suppressor cells in tumor-bearing mice. *J. Leukoc. Biol.* 91: 167–181.
48. Fridlender, Z. G., J. Sun, I. Mishalian, S. Singhal, G. Cheng, V. Kapoor, W. Horng, G. Fridlender, R. Bayuh, G. S. Worthen, and S. M. Albelda. 2012. Transcriptomic analysis comparing tumor-associated neutrophils with granulocytic myeloid-derived suppressor cells and normal neutrophils. *PLoS ONE* 7: e31524.
49. Gabrilovich, D. I., M. P. Velders, E. M. Sotomayor, and W. M. Kast. 2001. Mechanism of immune dysfunction in cancer mediated by immature Gr-1+ myeloid cells. *J. Immunol.* 166: 5398–5406.
50. Dolcetti, L., E. Peranzoni, S. Ugel, I. Marigo, A. Fernandez Gomez, C. Mesa, M. Geilich, G. Winkels, E. Traggiai, A. Casati, et al. 2010. Hierarchy of immunosuppressive strength among myeloid-derived suppressor cell subsets is determined by GM-CSF. *Eur. J. Immunol.* 40: 22–35.
51. Corzo, C. A., T. Condamine, L. Lu, M. J. Cotter, J. I. Youn, P. Cheng, H. I. Cho, E. Celis, D. G. Quiceno, T. Padhya, et al. 2010. HIF-1α regulates function and differentiation of myeloid-derived suppressor cells in the tumor microenvironment. *J. Exp. Med.* 207: 2439–2453.